

# The simplest 4-D chaotic system with line of equilibria, chaotic 2-torus and 3-torus behaviour

Jay Prakash Singh · B. K. Roy

Received: 8 September 2016 / Accepted: 27 April 2017 / Published online: 12 May 2017  
© Springer Science+Business Media Dordrecht 2017

**Abstract** The paper reports the simplest 4-D dissipative autonomous chaotic system with line of equilibria and many unique properties. The dynamics of the new system contains a total of eight terms with one nonlinear term. It has one bifurcation parameter. Therefore, the proposed chaotic system is the simplest compared with the other similar 4-D systems. The Jacobian matrix of the new system has rank less than four. However, the proposed system exhibits four distinct Lyapunov exponents with (+, 0, −, −) sign for some values of parameter and thus confirms the presence of chaos. Further, the system shows chaotic 2-torus (+, 0, 0, −), quasi-periodic [(0, 0, −, −), (0, 0, 0, −)] and multistability behaviour. Bifurcation diagram, Lyapunov spectrum, phase portrait, instantaneous phase plot, Poincaré map, frequency spectrum, recurrence analysis, 0–1 test, sensitivity to initial conditions and circuit simulation are used to analyse and describe the complex and rich dynamic behaviour of the proposed system. The hardware circuit realisation of the new system validates the MATLAB simulation results. The new system is developed from the well-known Rossler type-IV 3-D chaotic system.

**Keywords** Line of equilibria · Many equilibria · New chaotic system · Simplest chaotic system · Chaotic 2-torus

## 1 Introduction

A recent trend of chaos theory is devoted to the development of new chaotic systems which have unique features and unusual behaviours. The behaviours of a dynamical (chaotic/hyperchaotic) system are characterised by its equilibrium points [1]. Many recent papers are reported based on the properties of equilibrium points [1–7]. Hence, developing a new chaotic system which has unique features and unusual behaviours is the motivation of this paper.

The available chaotic or hyperchaotic systems are mainly categorised into two parts. These are self-excited attractors and hidden attractors [8]. The widely known chaotic systems like Lorenz [9], Lu [10], Chen [11] systems and system in [12, 13], etc. belong to self-excited attractors. These attractors have basin of attractions associated with the unstable equilibrium points. However, in case of hidden attractors, basin of attraction does not intersect with any small neighbourhood of any equilibrium points [14]. The analytical investigation, numerical localisation and computation of the hidden chaotic attractors are more difficult compared with the self-excited attractors [15–17]. The localisations of the hidden chaotic Chua attractors are discussed in [16, 17]. The control of multistability in the

---

J. P. Singh (✉) · B. K. Roy  
National Institute of Technology Silchar, Silchar, India  
e-mail: jayprakash1261@gmail.com

B. K. Roy  
e-mail: bkrmits@gmail.com

**Table 1** Categorisation of the 4-D hyperchaotic/chaotic systems with many number of equilibria

Sl. no.	Chaotic/hyperchaotic	Nature of system	References	No. of terms
1.	4-D Chaotic system	Plane of equilibria	[5]	Seven terms with five nonlinear terms
2.	4-D Chaotic system	Line of equilibria	This work	Eight terms with one nonlinear term
3.	4-D Hyperchaotic system	Line of equilibria	[30,31]	Nine terms with five nonlinear terms [31] Eight terms with five nonlinear terms [30]
4.	4-D Hyperchaotic system	Curve of equilibria	[32]	Eleven terms with three nonlinear terms
5.	4-D Memristive hyperchaotic system	Line of equilibria	[35,36]	Ten terms with five nonlinear terms [35] Nine terms with two nonlinear terms [36]

hidden chaotic attractors is reported in [18]. Hidden chaotic attractors are appeared in many applications like in induction motor with bound rotor [19], in convective fluid motion in rotating cavity [20]. The system which has no equilibrium point or only stable equilibrium points or a line of equilibria attractors is the type of hidden attractor [5, 8, 21–25]. Some recent category of hidden attractor is reported with only unstable node equilibrium point in a chaotic system [24].

Usually chaotic or hyperchaotic system has countable number of equilibria; one equilibrium point [26], two equilibrium points [27], three equilibrium points [9] or four equilibrium points [28]. Recently some chaotic or hyperchaotic systems are reported with many equilibrium points like [29, 30]. Some papers are available on these types of systems. Few papers are available on system which has line of equilibria [2, 31, 32]. A 3-D system with curve of equilibria is reported in [33]; a 3-D system with surface of equilibria is reported in [7]; [3, 34] reported a 3-D system with circle of equilibria. Very recently, a 4-D chaotic system with plane of equilibria is reported in [5]. However, most of the reported systems with many number of equilibria are derived from a general algebraic expression [2, 3, 5, 8, 25, 29, 33, 34] using extensive numerical search. The reported 4-D systems with many number of equilibria are summarised in Table 1. Thus, developing the simplest new 4-D chaotic system from a conventional chaotic system which has many number of equilibria (line of equilibria) with unique properties is still a challenging task.

In this paper, the simplest 4-D chaotic system with line of equilibria is reported. The system is different from the category of the rare attractor, or new category of rare attractor [5, 37, 38]. In the proposed system, the basin of attraction of the chaotic attractor intersect the

line of equilibria, but some point of basin of attraction may not intersect the line of equilibria. Here, the attractors are generated by choosing arbitrary initial conditions. The proposed system may consider as a new category of hidden attractor. The new system is derived from Rossler type-IV 3-D chaotic system [39]. Following points explain the interesting and unique properties of the proposed 4-D chaotic system:

1. The system has a line of equilibria and is derived from type-IV Rossler 3-D chaotic system [39].
2. The system has only one nonlinear term and a total of eight terms. Thus, the system is the simplest compared with similar available 4-D chaotic or hyperchaotic systems which have many equilibria. This claim is validated from Table 1. Although the system in [5] has seven terms, it consists of five nonlinear terms.
3. The rank of the Jacobian matrix is less than four. However, the system has four distinct Lyapunov exponents for some values of the parameters. Thus, the system behaves as a 4-D system with those values of parameters.
4. The system has chaotic 2-torus nature of Lyapunov exponents. Such nature of a dissipative chaotic system is rare in the literature.
5. The system shows 3-torus and 2-torus (quasi-periodic) and periodic responses other than the chaotic behaviour. The system also exhibits multistability (i.e., coexistence of attractors).
6. The system has asymmetry to its coordinates, planes and spaces. It has only one bifurcation parameter. Asymmetry indicates more disorderness and randomness of the system than to symmetry [40].

The above points also reflect the novelty and contributions of the proposed chaotic system. In 2011

[41] proposed three standard criteria for publication of a new system. These three criteria are as follows [5,41]:

1. The system should report an important unsolved problem in the literature.
2. The system should exhibit novel behaviour which is not available in the literature.
3. The system should be simple than the similar types of available system.

It is to be noted that a new system should satisfy at least one of the above criteria. Here, the proposed system in this paper satisfies both the second and third conditions. Many tools are used for analysis of a chaotic system. The following tools are used to analyse the proposed chaotic system: bifurcation diagram, Lyapunov spectrum, phase portrait, instantaneous phase plot, Poincaré map, frequency spectrum, recurrence analysis, 0–1 test, sensitivity to initial conditions and hardware circuit realisation.

The rest part of the paper is organised as follows. Section 2 describes the dynamics of the proposed system. The theoretical analyses of the system are presented in Sect. 3. Section 4 describes the numerical findings of the system. The sensitivity to initial conditions of the proposed system is discussed in Sect. 5. Section 6 describes the experimental circuit design and hardware circuit realisation of the proposed system. Finally, conclusions are presented in Sect. 7.

## 2 Dynamics of the new 4-D chaotic system

In 1979, Rossler proposed some sets (proto types) of chaotic systems [39]. The dynamics of the Rossler type-IV chaotic system is described as:

$$\begin{cases} \dot{x}_1 = -x_2 - x_3 \\ \dot{x}_2 = x_1 \\ \dot{x}_3 = a(x_2 - x_2^2) - bx_3 \end{cases} \quad (1)$$

where  $x_1, x_2, x_3$  are the state variables. The system exhibits chaotic behaviour with  $a = 0.386$ ,  $b = 0.2$ . System (1) produces attractors for the initial conditions  $x(0) = (0.7, -0.6, -0.7)^T$  and has two equilibrium points  $E_1(0, 0, 0)$  and  $E_2(0, 1.518, -1.581)$ . The variable  $x(0)$  is the vector of the initial condition of states of system (1) used for numerical simulation. A new 4-D

chaotic system is developed by introducing a state feedback control to the second state equation. The dynamics of the new chaotic system is described as:

$$\begin{cases} \dot{x}_1 = -x_2 - x_3 \\ \dot{x}_2 = x_1 - x_4 \\ \dot{x}_3 = a(x_2 - x_2^2) - bx_3 \\ \dot{x}_4 = cx_2 \end{cases} \quad (2)$$

where  $a, b, c$  are the parameters and  $x_1, x_2, x_3, x_4$  are the state variables. Here in system (2), the parameters  $a = b = 0.5$  are kept fixed. But  $c$  is considered as the bifurcation parameter. This is because of the fact that the parameters  $a$  and  $b$  are the parameters of the original system and parameter  $c$  is the parameter of the new system. Hence, to see the effect of the new parameters on the new system, it is considered as the bifurcation parameter. However, the parameters  $a$  and  $b$  are also varied to see their effect, i.e., different dynamical responses of the new system. The results of variation of parameters  $a, b$  and  $c$  in bifurcation diagram and Lyapunov spectrum are discussed in the numerical finding section. In this paper, all the simulations are carried out using *ode* – 45 solver in MATLAB simulation environment with initial conditions  $x(0) = (0.01, 0.001, 0.001, 0.1)^T$ . Detailed theoretical and numerical analyses of system (2) are presented in subsequent sections.

## 3 Theoretical findings

In this section, some theoretical analyses of the proposed system are presented using dissipativity property, symmetrical property and equilibrium points analyses.

### 3.1 Dissipative and symmetrical property

The divergence of system (2) is described as

$$\nabla V = \frac{\partial \dot{x}_1}{\partial x_1} + \frac{\partial \dot{x}_2}{\partial x_2} + \frac{\partial \dot{x}_3}{\partial x_3} + \frac{\partial \dot{x}_4}{\partial x_4} = -b \quad (3)$$

Thus, system (2) is dissipative for  $b > 0$ . The proposed system has rate of state space contraction equal to  $-1/2$  for  $b = 0.5$ . The system has no trajectories going to infinity as  $t \rightarrow \infty$ . The dissipativity property of a system gives existence of bounded global attractor

and analytical localisation of the global attractor in the phase space [42].

The boundedness of the chaotic trajectories of system (2) is proved using the following theorem. The boundedness of a chaotic system using the similar approach can be seen in [6, 43].

**Theorem 1** *Suppose that parameters  $a$ ,  $b$  and  $c$  of system (2) are positive. Then, the orbits of system (2) including chaotic orbits are confined in a bounded region.*

*Proof* Consider a Lyapunov function candidate as in (4)

$$v(x_1, x_2, x_3, x_4) = \frac{1}{2} [cx_1^2 + cx_2^2 + x_3^2 + x_4^2] \quad (4)$$

The time derivative of (4) is given as

$$\dot{v}(x_1, x_2, x_3, x_4) = cx_1\dot{x}_1 + cx_2\dot{x}_2 + x_3\dot{x}_3 + x_4\dot{x}_4 \quad (5)$$

Using system dynamics (2), (5) can be written as

$$\begin{aligned} \dot{v}(x_1, x_2, x_3, x_4) &= -cx_1x_3 + ax_2x_3 - ax_2^2x_3 - bx_3^2 \\ &= -\left(\frac{c}{2\sqrt{b}}x_1 + \sqrt{b}x_3\right)^2 \\ &\quad + \frac{c^2}{4b}x_1^2 - \left(\sqrt{ax_3}x_2 - \frac{\sqrt{ax_3}}{2}\right)^2 \\ &\quad + \frac{a}{4}x_3^2 \end{aligned}$$

Let  $R_0$  be the sufficiently large region so that for all trajectories  $(x_1, x_2, x_3, x_4)$  satisfy

$$v(x_1, x_2, x_3, x_4) = R \quad \text{for } R > R_0$$

with the following condition

$$\begin{aligned} &\left[\left(\frac{c}{2\sqrt{b}}x_1 + \sqrt{b}x_3\right)^2 + \left(\sqrt{ax_3}x_2 - \frac{\sqrt{ax_3}}{2}\right)^2\right. \\ &\quad \left. > \frac{c^2}{4b}x_1^2 + \frac{a}{4}x_3^2\right] \end{aligned}$$

Consequently on the surface

$$\{(x_1, x_2, x_3, x_4) | v(x_1, x_2, x_3, x_4) = R\}.$$

Since,  $R > R_0$  we can write,

$$v(x_1, x_2, x_3, x_4) < 0,$$

or we can say that, the set

$$\{(x_1, x_2, x_3, x_4) | v(x_1, x_2, x_3, x_4) \leq R\}$$

is a confined region for all the trajectories of system (2).  $\square$

The system is not invariant under any coordinate, plane and space transformation. Thus, the system is asymmetrical to its coordinates, planes and spaces.

### 3.2 Equilibria and eigenvalues

The equilibria of system (2) can be found by equating each state equation to zero. The equilibria of system (2) are  $E = (x_1^*, 0, 0, x_1^*)$ . Thus, it is clear that system (2) has a line of equilibria. The eigenvalues and stability corresponding to the equilibria  $E$  can be found by using the Jacobian matrix. The Jacobian matrix of proposed system (2) at equilibria  $E$  is given in (6).

$$J = \begin{bmatrix} 0 & -1 & -1 & 0 \\ 1 & 0 & 0 & -1 \\ 0 & a & -b & 0 \\ 0 & c & 0 & 0 \end{bmatrix} \quad (6)$$

The characteristic equation of (6) is

$$\lambda(\lambda^3 + k_1\lambda^2 + k_2\lambda + k_3) = 0 \quad (7)$$

where  $k_1 = b$ ,  $k_2 = c$ ,  $k_3 = bc$ . It is clear that there is a zero eigenvalue for all equilibrium points of system (2). The eigenvalues and their corresponding eigenvectors of the system for  $a = b = 0.5$ ,  $c = 0.014$  are given in Table 2. A comparison between the proposed system and the Rossler type-IV chaotic systems is given in Table 3. The proposed system belongs to the category of the hidden attractors since it has line of equilibria [44, 45].

### 4 Numerical findings

The dynamic behaviours of a self-excited chaotic or hyperchaotic system (having countable equilibrium points) can be obtained with the knowledge of location of equilibria or by considering initial conditions near a equilibrium point. However, for a system with a line of equilibria, it is difficult to obtain the dynamic behaviours with the knowledge of the location of equilibria. The dynamic behaviours of the proposed system are analysed using numerical findings. In this section, different numerical tools are used to analyse the complex dynamic behaviours of the proposed system.

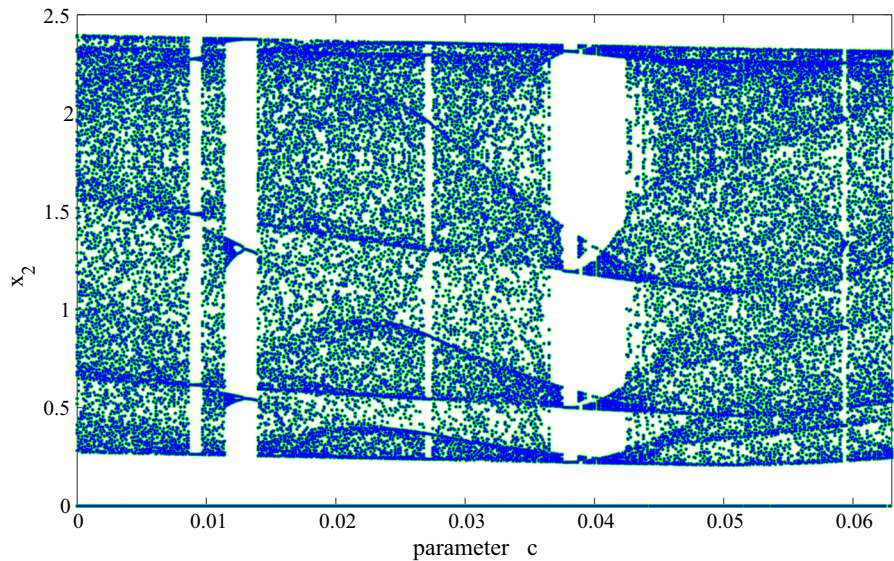
**Table 2** The eigenvalues and their corresponding eigenvectors of the new system with  $c = 0.014$  at equilibria  $E$

Sl. no.	Eigenvalues	Eigenvectors
1	$\lambda_1 = 0.1509 + 1.1105i$	$(0.7186, 0.0892 - 0.6420i, -0.1976 - 0.1560i, -0.0078 - 0.0022i)$
2	$\lambda_2 = 0.1509 - 1.1105i$	$(0.7186, 0.0892 + 0.6420i, -0.1976 + 0.1560i, -0.0078 + 0.0022i)$
3	$\lambda_3 = -0.8018$	$(-0.3898, -0.4758, 0.7884, 0.0083)$
4	$\lambda_4 = 0$	$(0.7071, 0, 0, 0.7071)$

**Table 3** Comparison between Rossler type-IV and the new system

Sl. no.	Property	System (1)	System (2)
1	Divergence	$\nabla v < 0$	$\nabla v < 0$
2	Symmetrical	Asymmetry	Asymmetry
3	Equilibrium point	Two	Infinite number (line of equilibria)
4	Dynamical behaviour	Chaotic, periodic, quasi-periodic	Chaotic, chaotic 2- torus, periodic, quasi-periodic
5	Types of attractors	Self-excited attractors	Hidden attractors
6	Lyapunov dimension ( $D_{KY}$ )	$2 < D_{KY} < 2.1$	$3 < D_{KY} < 3.2$

**Fig. 1** Bifurcation diagram of system (2) with  $c \in [0.0, 0.0629]$  and  $a = b = 0.5$



4.1 Bifurcation and Lyapunov spectrum analyses

The dynamic behaviour of the proposed system for other values of the bifurcation parameter is analysed using bifurcation diagram and Lyapunov spectrum. Both the plots are obtained by variation of one parameter while keeping other fixed. Lyapunov spectrum is obtained using Lyapunov exponents for different values of parameter. Lyapunov exponents are obtained by using Wolf algorithm [46] with observation time  $T = 10,000$  and sampling size  $\Delta t = 0.002$ .

The bifurcation diagram of the proposed system with a variation of parameter  $c \in [0.0, 0.0629]$  and  $c \in [0.063, 0.26]$  keeping other parameters fixed are shown in Figs. 1 and 2, respectively. Lyapunov spectrum of the proposed system with the variation of parameter  $c \in [0.0, 0.0629]$  and  $c \in [0.063, 0.26]$  and keeping other parameters fixed are shown in Figs. 3 and 4, respectively. Both the bifurcation diagrams of the system are generated with 10,000 observation time but discarding initial  $T = 9600$  transient time signal, step size  $\Delta t = 0.01$  and fixed initial conditions  $x(0) =$

**Fig. 2** Bifurcation diagram of system (2) with  $c \in [0.063, 0.25]$  and  $a = b = 0.5$

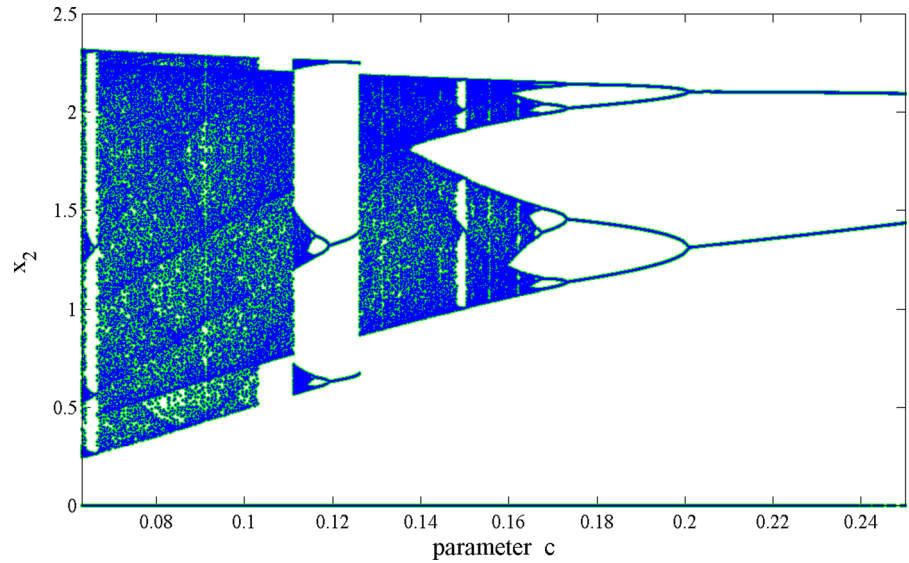


**Fig. 3** Lyapunov spectrum of system (2) with  $c \in [0.0, 0.0629]$  and  $x(0) = (0.01, 0.001, 0.001, 0.1)^T$

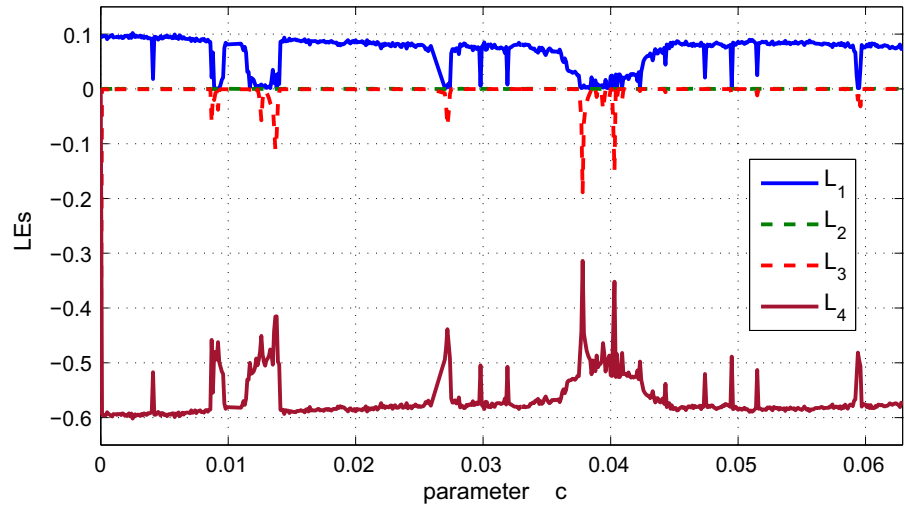


**Fig. 4** Lyapunov spectrum of system (2) with  $c \in [0.063, 0.25]$  and  $x(0) = (0.01, 0.001, 0.001, 0.1)^T$

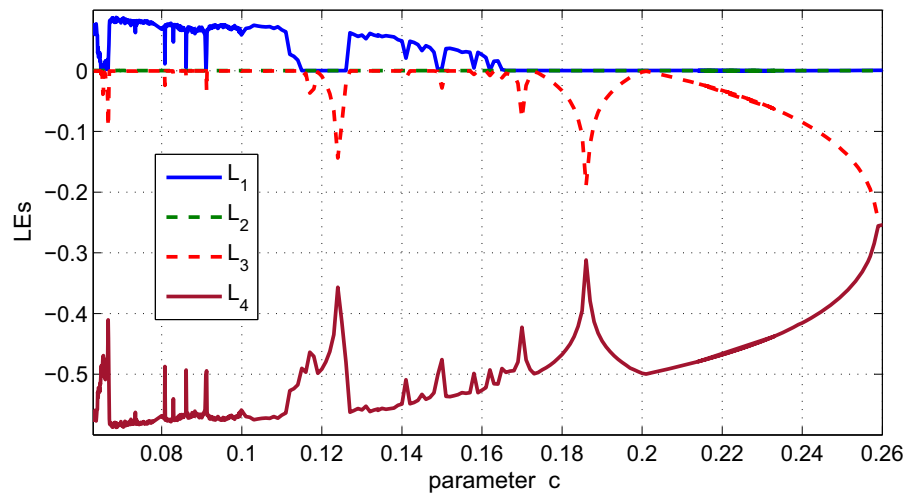


**Fig. 5** Lyapunov spectrum of system (2) with  $a \in [0.4, 0.5273]$ ,  $b = 0.5, c = 0.014$  and  $x(0) = (0.01, 0.001, 0.001, 0.1)^T$

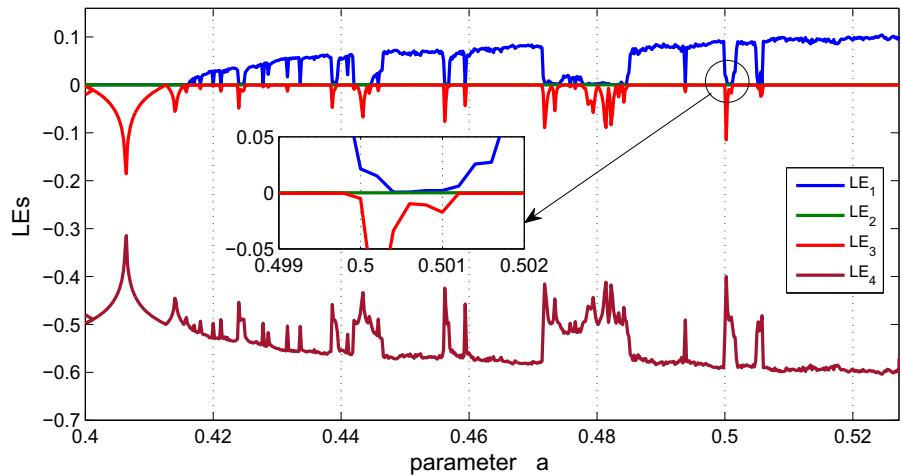
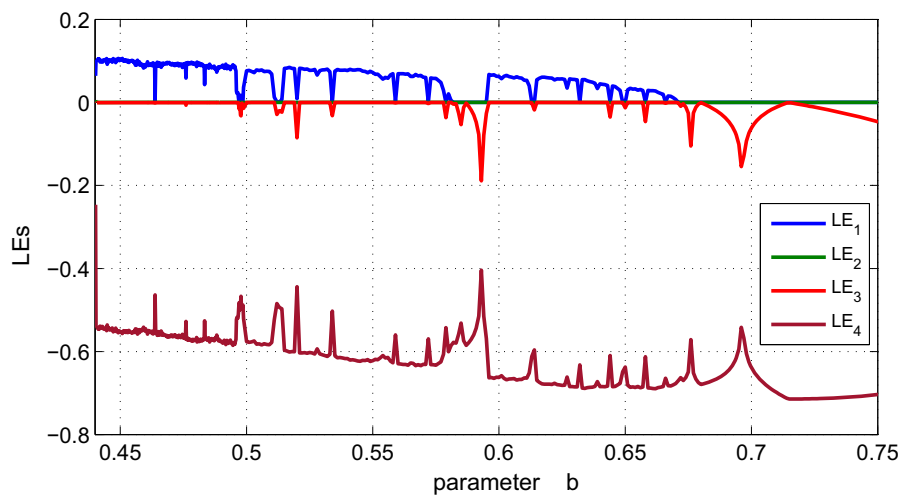


**Fig. 6** Lyapunov spectrum of system (2) with  $b \in [0.44, 0.75]$ ,  $a = 0.5, c = 0.014$  and  $x(0) = (0.01, 0.001, 0.001, 0.1)^T$



$(0.01, 0.001, 0.001, 0.1)^T$ . It is noted from these figures that the system produces chaotic, chaotic 2-torus and quasi-periodic behaviours (including 2-torus and 3-torus). The 2-torus quasi-periodic behaviour is considered when the nature of the Lyapunov exponents is  $(0, 0, -, -)$  and 3-torus is considered when the nature of Lyapunov exponents is  $(0, 0, 0, -)$ . The chaotic 2-torus is named when Lyapunov exponents are  $(+, 0, 0, -)$  as given in [47].

Lyapunov spectrum of system (2) with variation of parameters  $a$  and  $b$  but keeping  $b = 0.5, c = 0.014$  and  $a = 0.5, c = 0.014$  fixed are shown in Figs. 5 and 6, respectively. It is seen from Lyapunov spectrum plots that with the variation of parameters  $a$  and  $b$ , the new system has different dynamical behaviours like chaotic, chaotic 2-torus, quasi-periodic. It is also observed from

the Figs. 3, 4, 5 and 6 that the system has almost same ranges of parameters for chaotic behaviour. Lyapunov spectrum for variation of parameter  $c$  is shown up to  $a = 0.5237$  (Fig. 5). This is because the system response is unbounded after  $a > 0.5237$ . The same phenomenon is observed in case of the parameter  $b$  (Fig. 6) for  $b < 0.44$ .

The nature of Lyapunov exponents for chaotic and chaotic 2-torus behaviour of system (2) for some values of parameter  $c$  are given in Tables 4 and 5, respectively. It is seen from Table 4 that the system has four distinct Lyapunov exponents. This clearly establish that although the Jacobian matrix of the system has rank less than four, but the system behaves as four dimensional for some selected values of parameters. This fact is validated from reference [48].

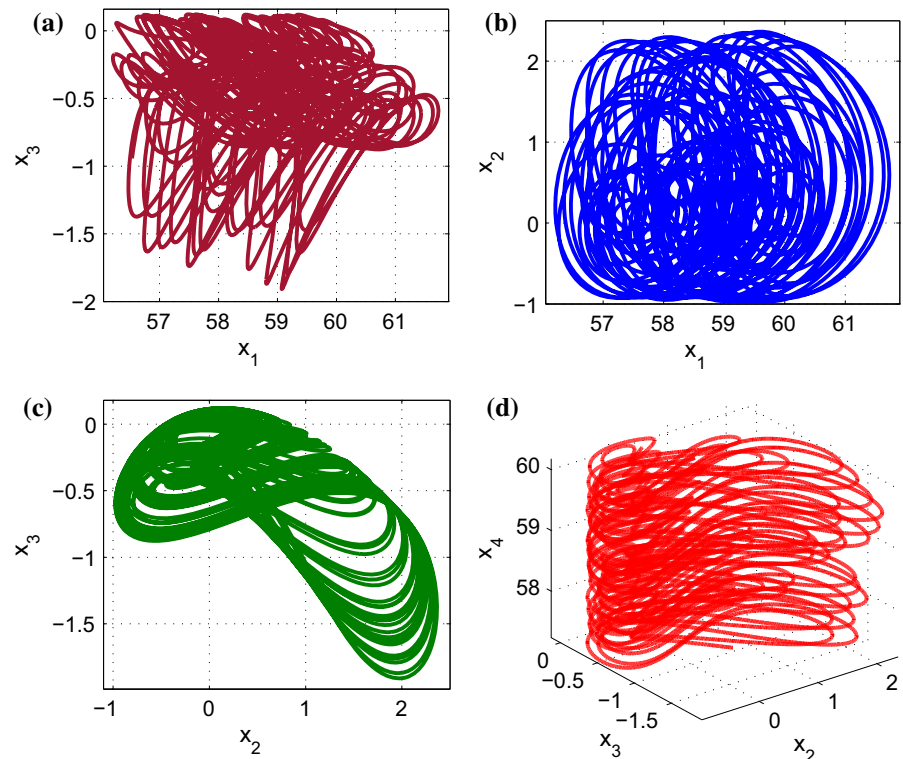
**Table 4** Four distinct nature of Lyapunov exponents (+, 0, −, −) (chaotic) for some values of parameter  $c$  of system (2)

Sl. no.	Parameter $c$	LE1	LE2	LE3	LE4	Summation of LEs
1.	$c = 0.014$	0.0191	0	−0.0050	−0.5141	−0.5
2.	$c = 0.0139$	0.0322	0	−0.0284	−.05038	−0.5
3.	$c = 0.0172$	0.0873	0	−0.0004	−0.5869	−0.5
4.	$c = 0.0235$	0.0775	0	−0.0004	−0.5771	−0.5
5.	$c = 0.0242$	0.0808	0	−0.0004	−0.5804	−0.5
6.	$c = 0.0306$	0.0837	0	−0.0003	−0.5834	−0.5
7.	$c = 0.037$	0.0290	0	−0.0007	−0.5283	−0.5

**Table 5** Three distinct nature of Lyapunov exponents (+, 0, 0, −) (chaotic 2-torus) for some values of parameter  $c$  of system (2)

Sl. no.	Parameter $c$	LE1	LE2	LE3	LE4	Summation of LEs
1.	$c = 0.0017$	0.0955	0	0	−0.5955	−0.5
2.	$c = 0.0052$	0.0956	0	0	−0.5956	−0.5
3.	$c = 0.0547$	0.0856	0	0	−0.5856	−0.5
4.	$c = 0.0499$	0.0838	0	0	−0.5838	−0.5

**Fig. 7** Chaotic attractors of system (2) with  $c = 0.014$  and  $x(0) = (0.01, 0.001, 0.001, 0.1)^T$



The chaotic attractors of system (2) are shown in Fig. 7. The attractors of the system are shown considering signal from for 9500 to 10,000 observation time. Thus, the attractors are bounded. The local Lyapunov

dimensions (LDs) of the points on the grid of the third attractor (Fig. 7c) of system (2) are shown in Fig. 8. The LDs are shown here only for the grid points where the system has chaotic behaviour. The system has max-



**Fig. 8** Local Lyapunov dimensions for chaotic behaviour on the grid points of the third attractor of system (2) with  $c = 0.014$

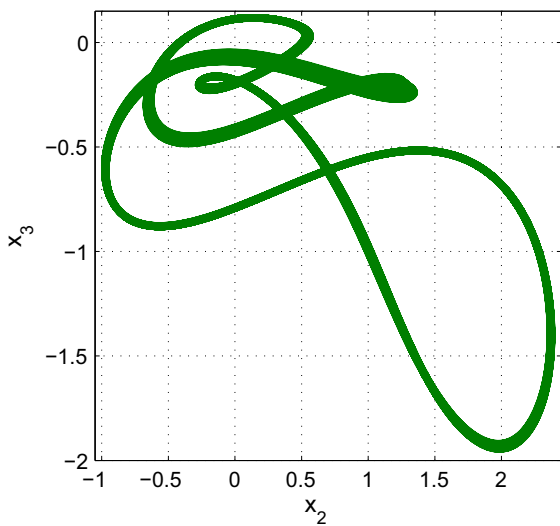
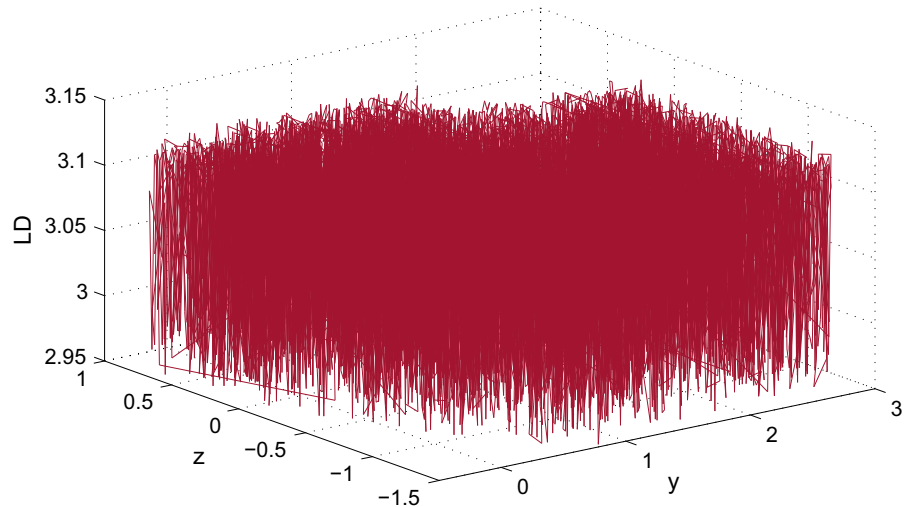


**Fig. 9** Quasi-periodic (3-torus) behaviour of system (2) with  $c = 0.0094$  and  $x(0) = (0.01, 0.001, 0.001, 0.1)^T$  where LEs are  $L_i = (0, 0, 0, -0.50)$

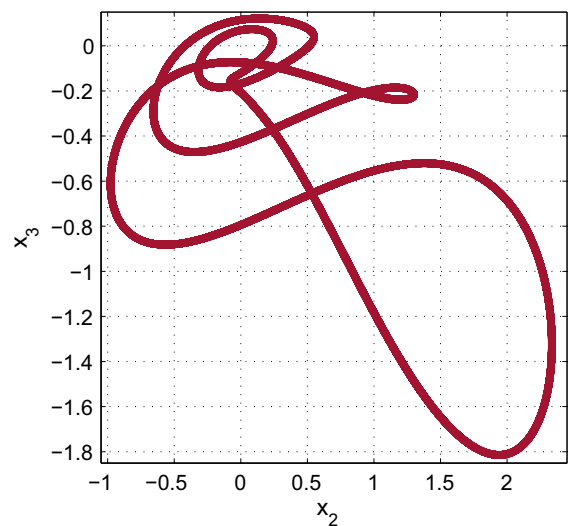


**Fig. 10** Quasi-periodic (2-torus) behaviour of system (2) with  $c = 0.0384$  and  $x(0) = (0.01, 0.001, 0.001, 0.1)^T$  where LEs are  $L_i = (0, 0, -0.0060, -0.4950)$

imum  $K_{DY}$  dimension equal to 3.1271 among the grid points of the third attractor of the system. The other behaviours of system (2) like 3-torus and 2-torus are shown in Figs. 9 and 10, respectively.

#### 4.2 Instantaneous phase and Poincaré map

To validate the chaotic dynamics of system (2), the instantaneous phase ( $\vartheta$ ) and Poincaré maps are plotted. The instantaneous phase ( $\vartheta$ ) is plotted using Hilbert transformation. Suppose, a chaotic signal  $x(t)$  is given

in the form of a complex signal  $s(t)$ , its amplitude ( $A$ ) and phase ( $\vartheta$ ) can be written as

$$s(t) = x(t) + i\tilde{x}(t) = A(t)e^{j\vartheta(t)} \tag{8}$$

where

$$\tilde{x}(t) = \frac{1}{\pi} P \cdot V \left( \int_{-\infty}^{\infty} \frac{x(\tau)}{t - \tau} d\tau \right) \tag{9}$$

where  $P \cdot V$  is the Cauchy principle value in the Hilbert transform (HT). Here, HT is calculated in MATLAB

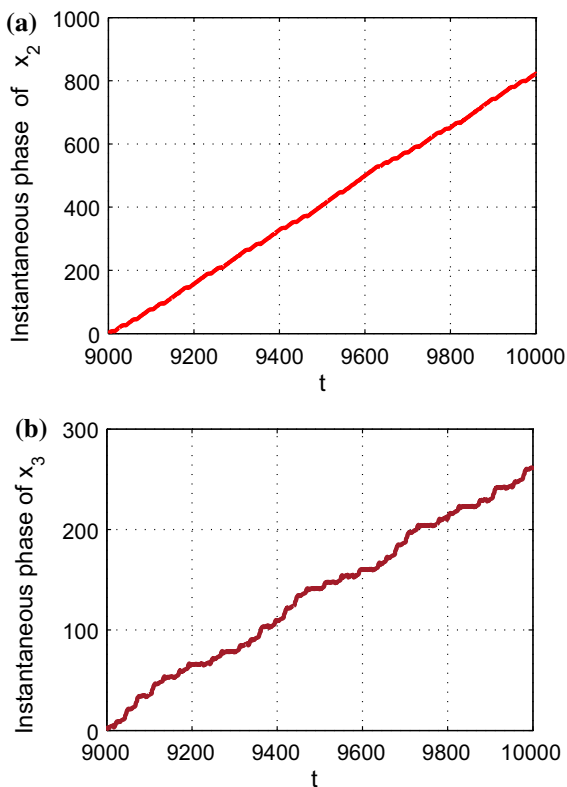


**Fig. 11** The instantaneous phase ( $\emptyset$ ) of the  $x_2$  and  $x_3$  signals of system (2) with  $c = 0.014$  and  $x(0) = (0.01, 0.001, 0.001, 0.1)^T$  and  $\Delta t = 0.001$  using HT

using the technique given in [49]. The instantaneous phase of  $x_2(t)$  and  $x_3(t)$  signals after truncating initial transient part are shown in Fig. 11. The instantaneous phase ( $\emptyset$ ) of a chaotic signal increases monotonically (inset) as the time increases [49, 50]. It is seen that the instantaneous phase ( $\emptyset$ ) of the system increases monotonically with time. The monotonous increase in the phase indicates the chaotic behaviour of the system.

The Poincaré maps on the different sections of the plane of system (2) are shown in Figs. 12 and 13. The maps in Figs. 12 and 13 are drawn for  $x_2 = 0$  and  $x_3 = 0$ , respectively. Different random dots in the Poincaré maps indicate the chaotic behaviour of the system [48]. Poincaré maps in Figs. 12 and 13 are generated for observation time in the ranges  $9500 < t < 10,000$ .

### 4.3 Frequency spectrum

The frequency spectra of system (2) are plotted to know the complex dynamic behaviour. The single sided fre-

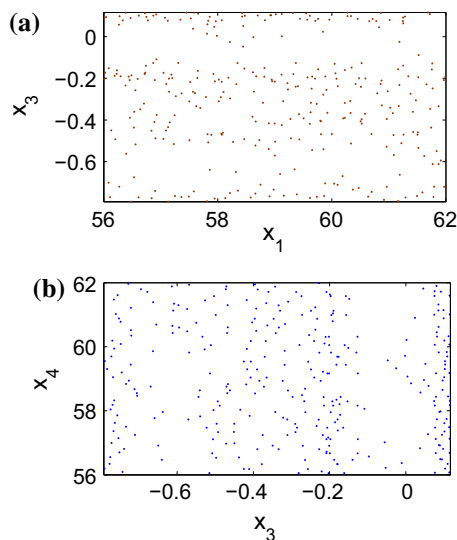


**Fig. 12** Poincaré maps on the plane of the system for  $x_2 = 0$  with  $c = 0.014$ ,  $x(0) = (0.01, 0.001, 0.001, 0.1)^T$  and  $\Delta t = 0.001$ : **a** on  $x_1 - x_3$  plane, **b** on  $x_3 - x_4$  plane

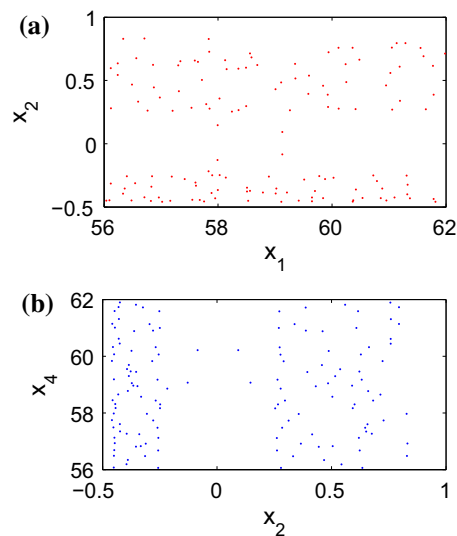


**Fig. 13** Poincaré maps on the plane of the system for  $x_3 = 0$  with  $c = 0.014$ ,  $x(0) = (0.01, 0.001, 0.001, 0.1)^T$  and  $\Delta t = 0.001$ : **a** on  $x_1 - x_2$  plane, **b** on  $x_2 - x_4$  plane

quency spectra of  $x_2(t)$  and  $x_3(t)$  signals of system (2) are shown in Fig. 14. Random peaks in the spectrum indicate the chaotic behaviour of the proposed system [48].

### 4.4 Recurrence analysis

A recurrence plot (RP) is a graphical visualisation of the repetitions or recurrences of a particular state of a

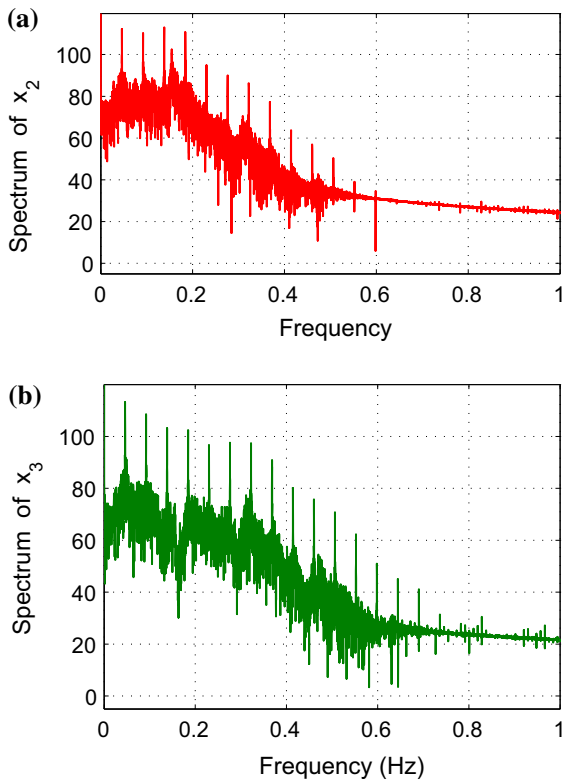


**Fig. 14** The frequency spectrum of system (2) with  $c = 0.014$  and  $x(0) = (0.01, 0.001, 0.001, 0.1)^T$  and  $\Delta t = 0.001$ : **a** spectrum of  $x_2(t)$  and **b** spectrum of  $x_3(t)$

system as its dynamics evolve [49]. It is used to study the reduced phase space plot of a higher dimensional system. In this the recurrence of a state at time  $i$  at a different time  $j$  is marked within a 2-D square matrix whose column and row correspond to a pair of time scales. The matrix is marked with the black and white dots (usually a black dots for recurrence). A signal  $x_1(t)$  is used from the multi-variable  $x(t) = [x_1(t), x_2(t), \dots, x_m(t)]$  to construct a lower n-D phase space using a time delay ( $\tau$ ). The reconstructed trajectory in n-D phase space can be written as [49].

$$w = [y_1, y_2, y_3, y_4]^T \tag{10}$$

where  $y_i = [x_i, x_{i+\tau}, \dots, x_{i+(D_E-1)\tau}]$  and  $m = n - (D_E - 1)\tau$  and  $D_E$  is the embedding dimension. Any recurrence of state  $i$  with state  $j$  can be expressed as [49];

$$R_{i,j}^\varepsilon = \Theta(\varepsilon - \|y_i - y_j\|) \tag{11}$$

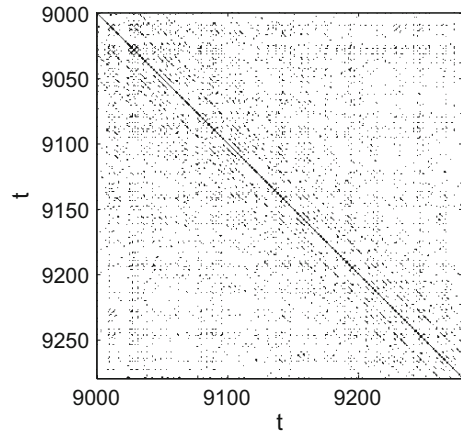


**Fig. 15** The recurrence plot of  $x_2(t)$  of system (2) with  $c = 0.014$  and  $x(0) = (0.01, 0.001, 0.001, 0.1)^T$ ,  $\Delta t = 0.001$ ,  $D_E = 6$ ,  $\tau = 75$ .

where  $\Theta$  is the Heaviside function and  $\varepsilon$  is an arbitrary threshold. Here,  $x_2(t)$  signal of system (2) is used for the recurrence plot. A total of 10,000 data points are used. The recurrence plot is obtained by assuming  $\varepsilon = 2$ ,  $D_E = 7$  and the time delay  $\tau = 75$ . The recurrence plot is shown in Fig. 15. The random distribution of the black dots indicates the chaotic behaviour [49]. The label of  $x$  and  $y$  in Fig. 15 is considered based on the theory given in [51,52].

#### 4.5 0–1 test analysis

It is a binary test used to classify the chaotic or periodic behaviour of a system [53]. Here, the dynamics of the system is plotted in a space of translation variable and asymptotic growth rate ( $k_c$ ) of the mean square displacement of the trajectories. The chaotic and periodic behaviours are defined based on the values of  $k_c$ . The translation variables are defined as [49,53,54]:

$$\begin{cases} p_c(n) = \sum_{j=1}^n x(j)\cos(jc) \\ q_c(n) = \sum_{j=1}^n x(j)\sin(jc) \end{cases} \tag{12}$$

where  $c$  is a randomly chosen variable constant in the range of  $(0 - 2\pi)$  and  $x(j)$  is the time series of any state variable of a dynamical system. If the dynamics is chaotic, then the space of translation variables is a random Brownian-like motion, whereas if the dynamics is regular then the space of the translation variables is a bounded motion. The mean square displacement  $M_c(n)$

**Fig. 16** The 0–1 test of  $x_2(t)$  of system (2) with  $c = 0.014$  and  $x(0) = (0.01, 0.001, 0.001, 0.1)^T$  and  $\Delta t = 1$ : **a** dynamics of the translation components  $(p_c(n), q_c(n))$ , **b** asymptotic growth rate  $(k_c)$  and **c** mean square displacement  $M_c(n)$

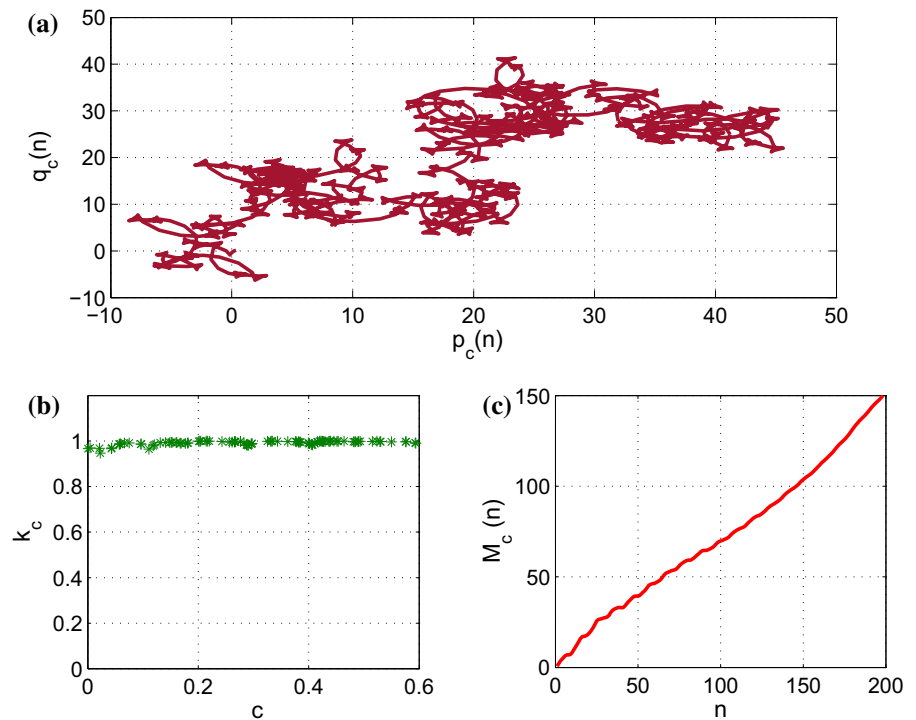
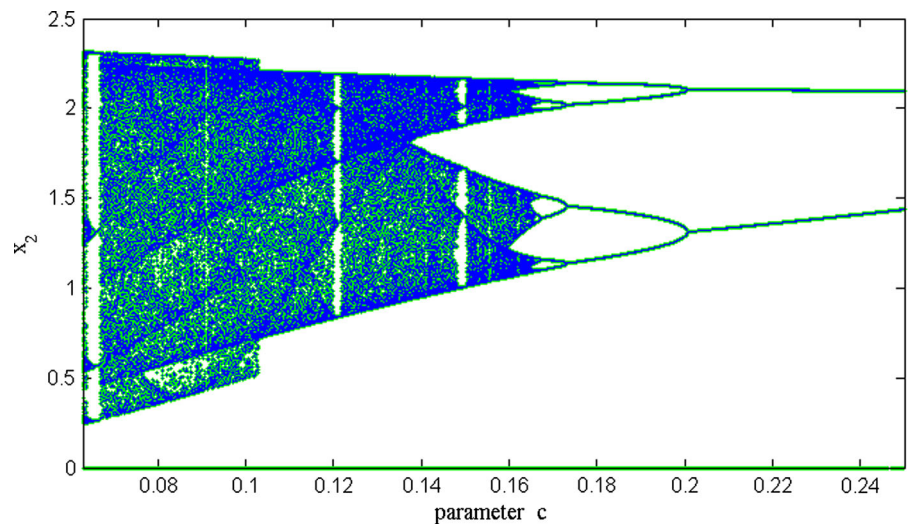


**Fig. 17** Bifurcation diagram of system (2) with  $a = b = 0.5$



obtained using translation variables  $(p_c(n), q_c(n))$  is defined as [49,53,54].

$$M_c(n) = \lim_{n \rightarrow \infty} \frac{1}{n} \sum_{j=1}^n \left\{ [p_c(j+n) - p_c(j)]^2 + [q_c(j+n) - q_c(j)]^2 \right\} \tag{13}$$

$M_c(n)$  grows exponentially for chaotic behaviour whereas it varies periodically for regular/periodic behaviour. The asymptotic growth rate  $(k_c)$  is defined as [49,53,54]

$$k_c = \lim_{n \rightarrow \infty} \frac{\log M_c(n)}{\log n} \tag{14}$$

**Fig. 18** **a** Coexistences of 2-torus with chaotic attractor and **b** coexistences of 2-torus with 2-torus of system (2) with  $a = b = 0.5, c = 0.12$

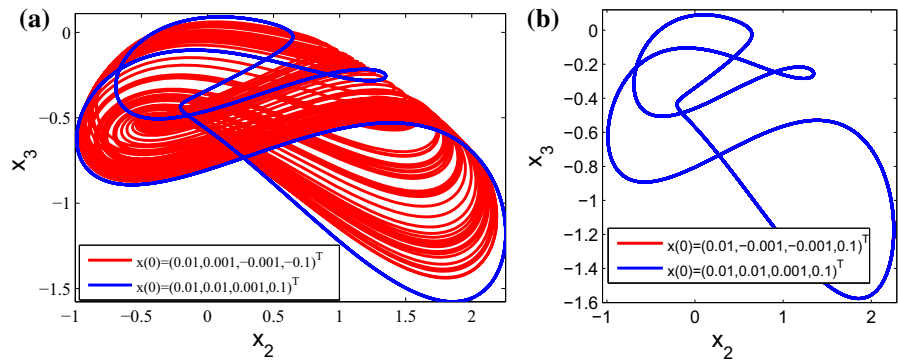
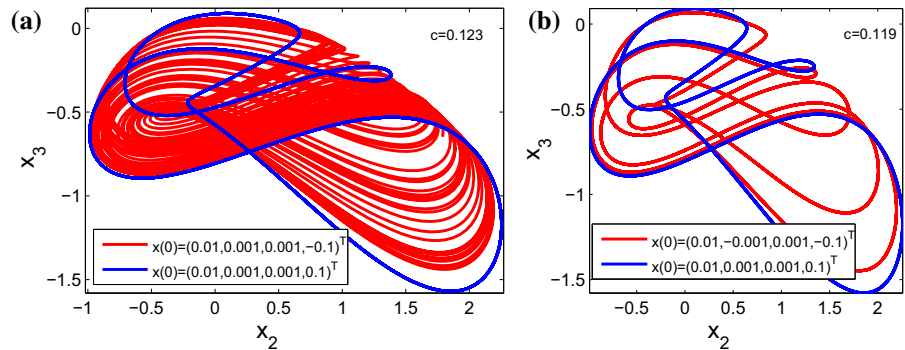


**Fig. 19** **a** Coexistence of 2-torus with chaotic attractor for  $c = 0.123$  and **b** coexistence of 2-torus with 3-torus with  $c = 0.119$  of system (2) with  $a = b = 0.5$



The value of  $k_c \approx 1$  determines the chaotic behaviour, and  $k_c \approx 0$  indicates the periodic/regular behaviour. Here,  $x_2(t)$  signal of system (2) is used for 0–1 test. The translation variables, asymptotic growth rate and mean square displacement are shown in Fig. 16. We got  $k_c = 0.99691 \approx 1$  for  $a = b = 0.5, c = 0.014$  which confirms the chaotic nature of the new system.

4.6 Multistability (coexistence of attractors)

Multistability can be determined by observing changes in the responses of bifurcation diagram of the system [55,56]. The bifurcation diagram of system (2) with variation of the parameter  $c$  is replotted to observe the phenomenon of multistability. The bifurcation diagram is plotted considering the final state for each value of  $c$  as the initial states for the next value of the bifurcation parameter. The results are shown in Fig. 17. It is observed by comparing Figs. 2 and 17 that the system has changed in behaviour for the bifurcation parameter range  $c \in [0.12, 0.14]$ . In Fig. 17, for  $c = 0.12$ , it appears that the system has chaotic behaviour, but in Fig. 2 it has periodic behaviour. It is also observed from Fig. 2 that for  $c \in [0.11, 0.125]$  the system has

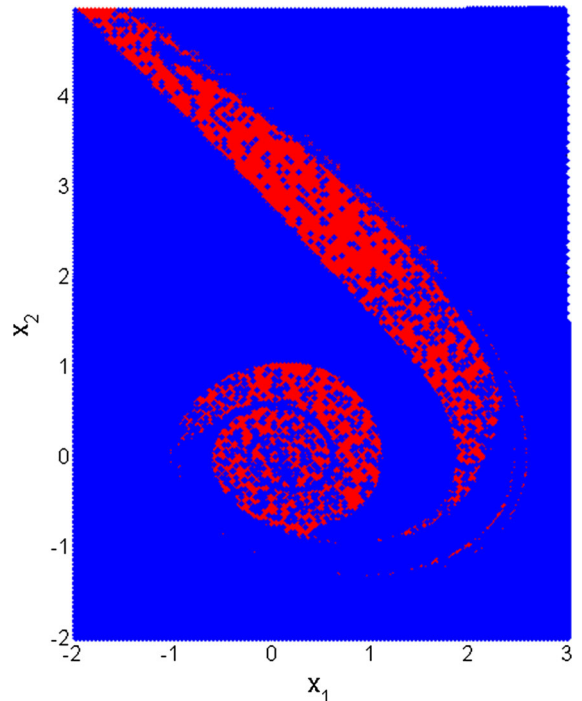


**Fig. 20** Sensitivity to initial conditions of system (2) with  $x_3 = 0.001, x_4 = 0.1$  and  $x_1 \in [-2, 3], x_2 \in [-2, 5]$  where red colour represents the chaotic nature and blue colour represents the unbounded nature of the proposed system. (Color figure online)

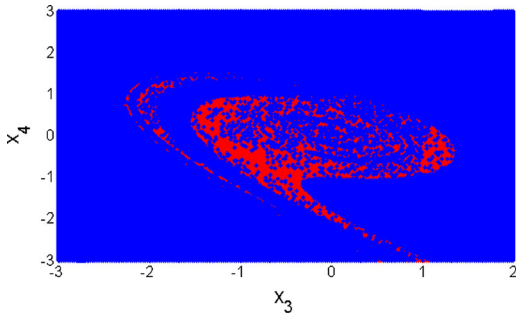
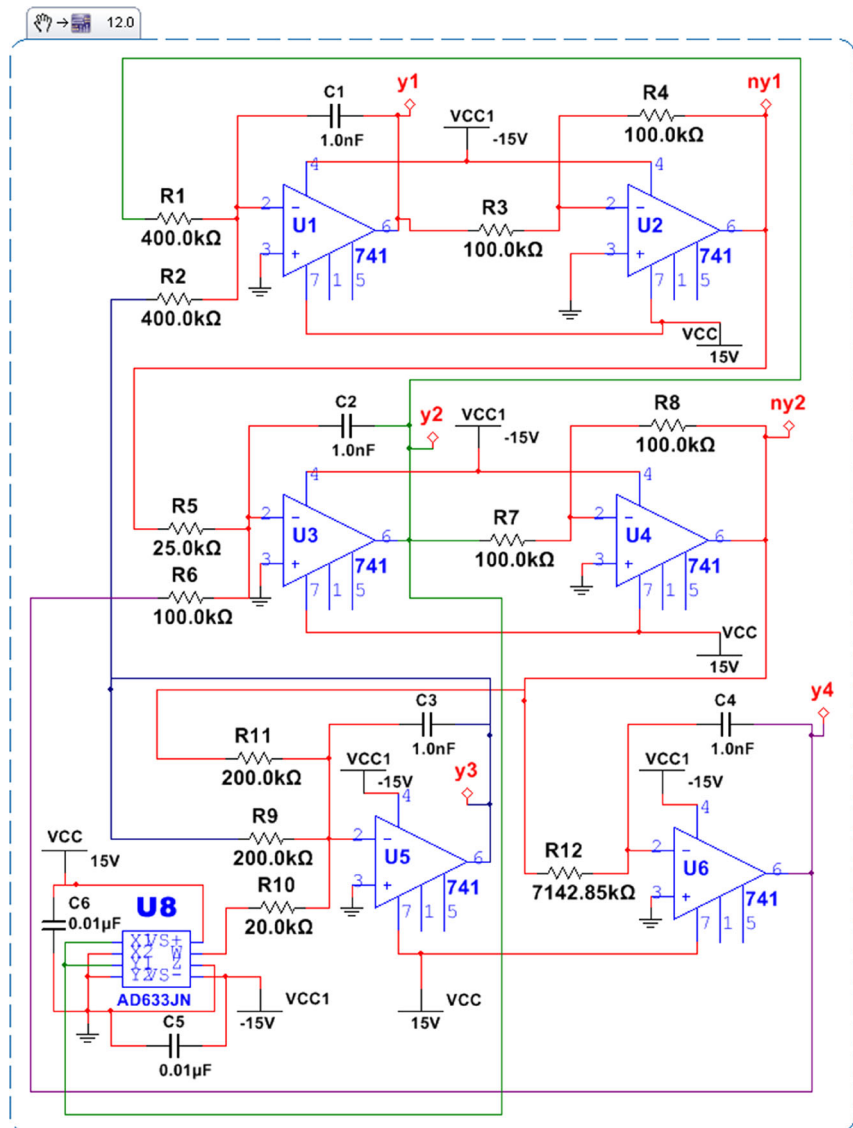


**Fig. 21** Sensitivity to initial conditions of system (2) with  $x_1 = 0.01$ ,  $x_2 = 0.001$  and  $x_3 \in [-3, 2]$ ,  $x_4 \in [-3, 3]$  where red colour represents the chaotic nature and blue colour represents the unbounded nature of the proposed system. (Color figure online)

**Fig. 22** Circuit design of chaotic system (2)



cascaded reverse period-doubling route to chaos along with one reverse period-doubling route to chaos, but in Fig. 17, there is no cascaded reverse periodic period-doubling route to chaos. Further in Fig. 17, there are four more jump routes to chaos. Thus, it seems that the system has coexistence of different attractors due to changes in initial conditions. The coexistences of (i) quasi-periodic (2-torus) with chaotic attractor and (ii) 2-torus with 2-torus of system (2) are shown in Fig. 18. The coexistences of (i) quasi-periodic (2-torus) with chaotic attractor and (ii) 2-torus with 3-torus of system (2) with  $c = 0.123$  and  $c = 0.119$ , respectively, are shown in Fig. 19.

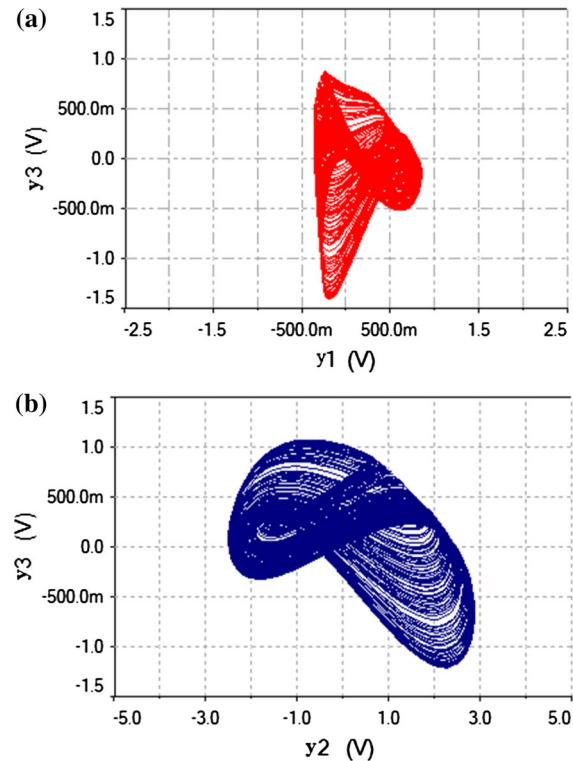


**Fig. 23** Chaotic attractors of system (2) using NI Multisim circuit simulation: **a** in  $y_1 - y_3$  plane with scale position 500, 500 mv/div and **b** in  $y_2 - y_3$  plane with scale position 1 V/div, 500 mv/div

## 5 Sensitivity to initial conditions

This section describes the effect of initial conditions on system (2).

System (2) is simulated with different initial conditions in the considered regions of four state variables. The results of two different cases are shown. In the first case, the initial conditions for state variables  $x_3(0) = 0.001$  and  $x_4(0) = 0.1$  are kept fixed and  $x_1(0)$  and  $x_2(0)$  are varied. In the second case, the state variables  $x_1(0) = 0.01$  and  $x_2(0) = 0.001$  are kept fixed, and  $x_3(0)$  and  $x_4(0)$  are varied. The simulated results for the first and second cases are shown in Figs. 20 and 21, respectively. It is seen from both the figures that system (2) is very sensitive to initial conditions.

## 6 Circuit validation

The circuit designed for the implementation of system (2) is shown in Fig. 22. The circuit validation of

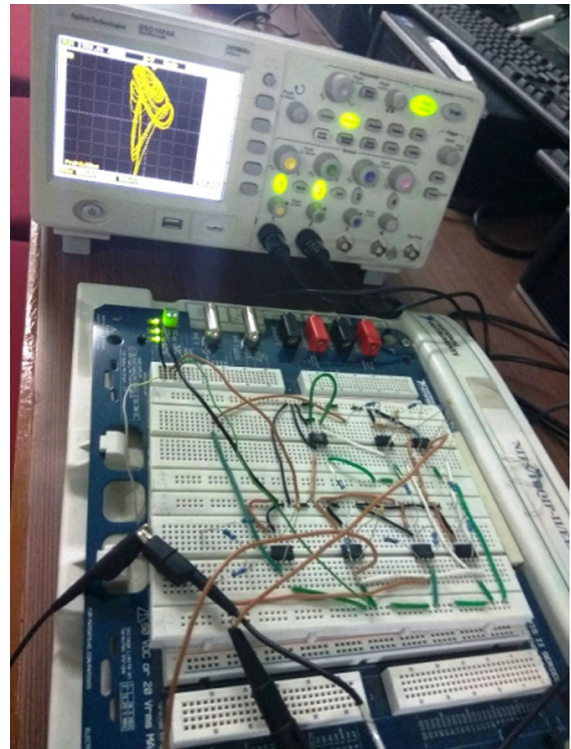


**Fig. 24** Hardware circuit design of system (2) on breadboard along with oscilloscope output

the new system is achieved using NI Multisim 12 software. Many chaotic circuits are simulated and verified using NI Multisim [57–61] and PSpice [62–65]. NI Multisim software is based on actual circuit components. Its simulation results are basically consistent with those of actual circuit results [58]. Here in circuit (Fig. 22), four integration lines are considered correspond to four states of the new system. The supply voltages are considered as  $\pm 15$  Vdc. The circuit is designed using four capacitors ( $C_1, C_2, C_3, C_4$ ), eleven resistances ( $R_1, \dots, R_{12}$ ), six op-amp (741) and one multiplier (AD633JN). Here, multiplier is used for the nonlinear term  $x^2$ . It is seen from the chaotic attractors plot (Fig. 7) of the new system that states  $x_1$  and  $x_4$  are in the range of 50 and 60. Thus, the states are scaled with  $y_1 = x_1/40$ ,  $y_2 = x_2/10$ ,  $y_3 = x_3/10$ ,  $y_4 = x_4/10$  to make compatible for the circuit simulation and implementable in the hardware circuit. The circuit equation corresponding to each state of scaled system (2) using Kirchhoff's laws can be obtained as:

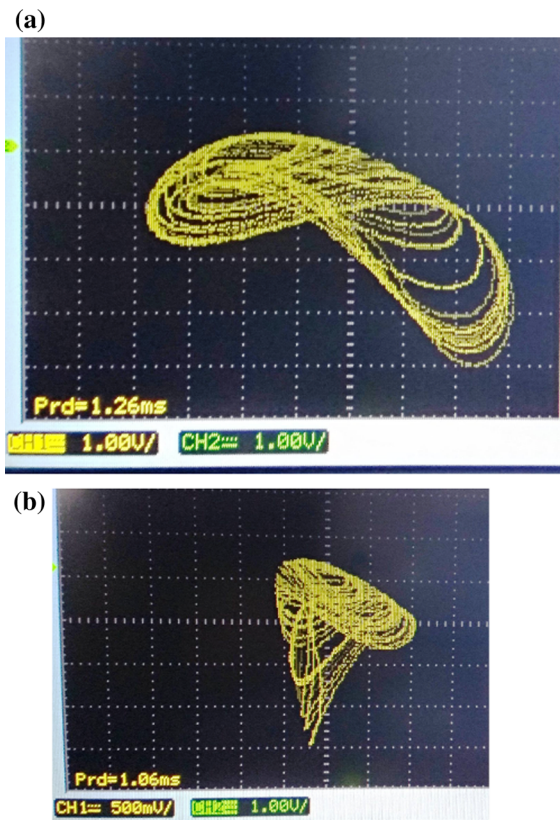


**Fig. 25** Chaotic attractors using hardware circuit realisation of system (2) in oscilloscope for: **a**  $x_2 - x_3$  plane and **b**  $x_1 - x_3$  plane

$$\begin{cases} \dot{y}_1 = \frac{1}{Rc_1} \left[ -\frac{R}{R_1}y_2 - \frac{R}{R_2}y_3 \right] \\ \dot{y}_2 = \frac{1}{Rc_2} \left[ \frac{R}{R_5}y_1 - \frac{R}{R_6}y_4 \right] \\ \dot{y}_3 = \frac{1}{Rc_3} \left[ \frac{R}{R_{11}}y_2 - \frac{0.1R}{R_{10}}y_2y_2 - \frac{R}{R_9}y_3 \right] \\ \dot{y}_4 = \frac{1}{Rc_4} \left[ \frac{R}{R_{12}}y_2 \right] \end{cases} \quad (15)$$

where the variables  $y_1, y_2, y_3, y_4$  are the outcomes of the integrators  $U1A, U3A, U5A, U6A$ . System (2) is equivalent to (15) with  $\tau = t/RC$ ,  $R_3 = R = R_4 = R_7 = R_8 = 100 \text{ k}\Omega$ ,  $R_{11} = \frac{R}{a} = 200 \text{ k}\Omega$ ,  $R_{10} = \frac{R}{a} = 20 \text{ k}\Omega$ ,  $R_1 = R_2 = 400 \text{ k}\Omega$ ,  $R_5 = 25 \text{ k}\Omega$ ,  $R_9 = \frac{R}{b} = 200 \text{ k}\Omega$ ,  $R_{12} = \frac{R}{c} = 7142.85 \text{ k}\Omega$ ,  $c_1 = c_2 = c_3 = c_4 = 1nF$  and  $a = b = 0.5$ ,  $c = 0.014$ . Hardware circuit design along with oscilloscope output results of system (2) is shown in Fig. 24. The chaotic attractors of system (2) with  $c = 0.014$  obtained using NI Multisim circuit simulation and hardware circuit realisation oscilloscope results are shown in Figs. 23

and 25, respectively. Agilent 1024A 200 MHz digital oscilloscope is used for capturing the experimental results. It is seen from Figs. 23 and 25 that the attractors plot using circuit simulation and hardware circuit realisation validate with the MATLAB simulation results.

## 7 Conclusions

In this paper, the simplest new 4-D chaotic system with the line of equilibria is reported. The system has only two types of behaviour. These are chaotic (chaotic, chaotic 2-torus) and quasi-periodic (2-torus, 3-torus). The system is unusual with many unique properties. The system exhibits multistability. The system has a total of eight terms including only one nonlinear term and one bifurcation parameter. Hence, the system is the simplest compared with similar 4-D systems (systems with many number of equilibria). The system has chaotic 2-torus with (+,  $\approx 0$ ,  $\approx 0$ , -) nature of Lyapunov exponents for chaotic behaviour which is rare in the literature. The rank of the Jacobian matrix of the proposed system is three which is less than the dimension of the system. However, the system exhibits four distinct Lyapunov exponents and thereby behaving as a 4-D system for some values of parameter. The system has asymmetry to its coordinates, plane and space. Bifurcation diagram, Lyapunov spectrum, phase portrait, instantaneous phase plot, Poincaré map, frequency spectrum, recurrence analysis, 0–1 test and theoretical analyses are used to analyse the complex dynamic behaviours of the proposed system. The simulation results using MATLAB are validated by using hardware circuit design and realisation. The design and analyses presented in this paper can be further extended by developing some new simplest 4-D/5-D hyperchaotic systems with new complex dynamical behaviours along with their applications.

**Acknowledgements** Author thanks editor and anonymous reviewers for their valuable suggestions that helped to improve the standard of the paper.

## References

1. Tahir, F.R., Jafari, S., Pham, V.-T., Volos, C., Wang, X.: A novel no-equilibrium chaotic system with multiwing butterfly attractors. *Int. J. Bifurc. Chaos* **25**(04), 1550056–1550067 (2015)



2. Jafari, S., Sprott, J.C.: Simple chaotic flows with a line equilibrium. *Chaos Solitons Fractals* **84**, 57–79 (2013)
3. Gotthans, T., Petrzela, J.: New class of chaotic systems with circular equilibrium. *Nonlinear Dyn.* **81**, 1143–1149 (2015)
4. Xu, Y., Zhang, M., Li, C.-L.: Multiple attractors and robust synchronization of a chaotic system with no equilibrium. *Optik Int. J. Light Electron Opt.* **127**(3), 1–5 (2015)
5. Jafari, S., Sprott, J.C., Molaie, M.: A simple chaotic flow with a plane of equilibria. *Int. J. Bifurc. Chaos* **26**, 1650098–1650104 (2016)
6. Yang, Q.: A chaotic system with one saddle and two stable node-foci. *Int. J. Bifurc. Chaos* **18**(5), 1393–1414 (2008)
7. Qi, G., Chen, G.: A spherical chaotic system. *Nonlinear Dyn.* **81**(3), 1381–1392 (2015)
8. Jafari, S., Sprott, J.C., Nazarimehr, F.: Recent new examples of hidden attractors. *Eur. Phys. J. Spec. Top.* **224**(8), 1469–1476 (2015)
9. Lorenz, E.N.: Deterministic nonperiodic flow. *J. Atmos. Sci.* **20**(2), 130–141 (1963)
10. Singh, P.P., Singh, J.P., Roy, B.K.: Synchronization and anti-synchronization of Lu and Bhalekar–Gejji chaotic systems using nonlinear active control. *Chaos Solitons Fractals* **69**, 31–39 (2014)
11. Chen, G., Ueta, T.: Yet another chaotic attractor. *Int. J. Bifurc. Chaos* **09**, 14651999–14652002 (1999)
12. Singh, J.P., Roy, B.K.: Crisis and inverse crisis route to chaos in a new 3-D chaotic system with saddle, saddle foci and stable node foci nature of equilibria. *Optik* **127**, 11982–12002 (2016)
13. Singh, J.P., Roy, B.K.: The nature of Lyapunov exponents is (+, +, ). Is it a hyperchaotic system? *Chaos Solitons Fractals* **92**, 73–85 (2016)
14. Wei, Z., Zhang, W.: Hidden hyperchaotic attractors in a modified Lorenz–Stenflo system with only one stable equilibrium. *Int. J. Bifurc. Chaos* **24**(10), 1450127–1450142 (2014)
15. Leonov, G.A., Kuznetsov, N.V.: Hidden attractors in dynamical systems: from hidden oscillations in Hilbert Kolmogorov, Aizerman, and Kalman problems to hidden chaotic attractor in chua circuits. *Int. J. Bifurc. Chaos* **23**(01), 1330002–1330010 (2013)
16. Leonov, G.A., Kuznetsov, N.V., Vagitsev, V.I.: Localization of hidden chaotic attractors. *Phys. Lett. A* **375**(23), 2230–2233 (2011)
17. Leonov, G.A., Kuznetsov, N.V., Vagitsev, V.I.: Hidden attractor in smooth chua systems. *Phys. D* **241**(18), 1482–1486 (2012)
18. Sharma, R., Shrimali, M.D., Prasad, A., Kuznetsov, N.V., Leonov, G.A.: Control of multistability in hidden attractors. *Eur. Phys. J. Spec. Top.* **224**(8), 1485–1491 (2015)
19. Leonov, G.A., Kuznetsov, N.V., Kiseleva, M.A., Solovyeva, E.P., Zaretskiy, A.M.: Hidden oscillations in mathematical model of drilling system actuated by induction motor with a wound rotor. *Nonlinear Dyn.* **77**(1–2), 277–288 (2014)
20. Leonov, G.A., Kuznetsov, N.V., Mokaev, T.N.: Hidden attractor and homoclinic orbit in Lorenz like system describing convective fluid motion in rotating cavity. *Commun. Nonlinear Sci. Numer. Simul.* **28**(1–3), 166–174 (2015)
21. Jafari, S., Sprott, J.C., Reza, M., Golpayegani, H.: Elementary quadratic chaotic flows with no equilibria. *Phys. Lett. A* **377**(9), 699–702 (2013)
22. Pham, V.T., Volos, C., Jafari, S., Wang, X.: Generating a novel hyperchaotic system out of equilibrium. *Optoelectron. Adv. Mater. Rapid Commun.* **8**(5–6), 535–539 (2014)
23. Pham, V.T., Volos, C., Jafari, S., Wei, Z., Wang, X.: Constructing a novel no equilibrium chaotic system. *Int. J. Bifurc. Chaos* **24**, 1450073–1450087 (2014)
24. Sprott, J.C., Jafari, S., Pham, V.T., Hosseini, Z.S.: A chaotic system with a single unstable node. *Phys. Lett. A* **379**(36), 2030–2036 (2015)
25. Sprott, J.C.: Strange attractors with various equilibrium. *Eur. Phys. J. Spec. Top.* **224**, 1409–1419 (2015)
26. Singh, J.P., Roy, B.K.: Analysis of an one equilibrium novel hyperchaotic system and its circuit validation. *Int. J. Control Theory Appl.* **8**(3), 1015–1023 (2015)
27. Singh, J.P., Roy, B.K.: A novel asymmetric hyperchaotic system and its circuit validation. *Int. J. Control Theory Appl.* **8**(3), 1005–1013 (2015)
28. Zhang, C.: Theoretical design approach of four-dimensional piecewise-linear multi-wing hyperchaotic differential dynamic system. *Optik* **127**(11), 1–6 (2016)
29. Wang, X., Chen, G.: Constructing a chaotic system with any number of equilibria. *Nonlinear Dyn.* **71**(3), 429–436 (2013)
30. Li, C., Sprott, J.C., Thio, W.: Bistability in a hyperchaotic system with a line equilibrium. *J. Exp. Theor. Phys.* **118**(3), 494–500 (2014)
31. Zhou, P., Yang, F.: Hyperchaos, chaos, and horseshoe in a 4D nonlinear system with an infinite number of equilibrium points. *Nonlinear Dyn.* **76**(1), 473–480 (2014)
32. Chen, Y., Yang, Q.: A new Lorenz-type hyperchaotic system with a curve of equilibria. *Math. Comput. Simul.* **112**, 40–55 (2015)
33. Kingni, S.T., Pham, V.-T., Jafari, S., Kol, G.R., Wofo, P.: Three-dimensional chaotic autonomous system with a circular equilibrium: analysis, circuit implementation and its fractional-order form. *Circuits Syst. Signal Process.* **35**, 1933–1948 (2016)
34. Jafari, S., Wang, X., Pham, V.-T., Ma, J.: A chaotic system with different shapes of equilibria. *Int. J. Bifurc. Chaos* **26**(04), 1–6 (2016)
35. Ma, J., Chen, Z., Wang, Z., Zhang, Q.: A four-wing hyperchaotic attractor generated from a 4-D memristive system with a line equilibrium. *Nonlinear Dyn.* **81**(3), 1275–1288 (2015)
36. Li, Q., Shiyi, H., Tang, S., Zeng, G.: Hyperchaos and horseshoe in a 4D memristive system with a line of equilibria and its implementation. *Int. J. Circuit Theory Appl.* **42**(11), 1172–1188 (2014)
37. Chudzik, A., Perlikowski, P., Stefanski, A., Kapitaniak, T.: Multistability and rare attractors in Van der Pol Duffing oscillator. *Int. J. Bifurc. Chaos* **21**(07), 1907–1912 (2011)
38. Klovov, A.V., Zakrzhevsky, M.V.: Parametrically excited pendulum systems with several equilibrium positions: bifurcation analysis and rare. *Int. J. Bifurc. Chaos* **21**, 2535–2825 (2011)
39. Rossler, O.E.: Continuous chaos: four prototype equations. *Ann. N. Y. Acad. Sci.* **316**, 376–392 (1979)
40. Qi, G., Chen, G., Zhang, Y.: On a new asymmetric chaotic system. *Chaos Solitons Fractals* **37**(2), 409–423 (2008)
41. Sprott, J.C.: A proposed standard for the publication of new chaotic systems. *Int. J. Bifurc. Chaos* **21**(9), 2391–2394 (2011)

42. Leonov, G.A., Kuznetsov, N.V., Mokaev, T.N.: Homoclinic orbits, and self-excited and hidden attractors in a Lorenz-like system describing convective fluid motion: homoclinic orbits, and self-excited and hidden attractors. *Eur. Phys. J. Spec. Top.* **224**(8), 1421–1458 (2015)
43. Nik, H.S., Golchaman, M.: Chaos control of a bounded 4D chaotic system. *Neural Comput. Appl.* **25**, 683–692 (2014)
44. Pham, V.-T., Jafari, S., Volos, C., Giakoumis, A., Vaidyanathan, S., Kapitaniak, T.: A chaotic system with equilibria located on the rounded square loop and its circuit implementation. *IEEE Trans. Circuits Syst. II Exp. Briefs* **63**(9), 878–882 (2016)
45. Dudkowski, D., Jafari, S., Kapitaniak, T., Kuznetsov, N.V., Leonov, G.A., Prasad, A.: Hidden attractors in dynamical systems. *Phys. Rep.* **637**, 1–50 (2016)
46. Wolf, A., Swift, J.B., Swinney, H.L., Vastano, J.A.: Determining Lyapunov exponents from a time series. *Phys. D* **16**, 285–317 (1985)
47. Parker, T.S., Chua, L.O.: *Practical Numerical Algorithms for Chaotic Systems*. Springer, Berlin (1989)
48. Li, C., Sprott, J.C., Thio, W., Zhu, H.: A new piecewise linear hyperchaotic circuit. *IEEE Trans. Circuits Syst. II Exp. Briefs* **61**(12), 977–981 (2014)
49. Sabarathinam, S., Thamilmaran, K.: Transient chaos in a globally coupled system of nearly conservative Hamiltonian Duffing oscillators. *Chaos Solitons Fractals* **73**, 129–140 (2015)
50. Salvino, L.W., Pines, D.J., Todd, M., Nichols, J.M.: *EMD and Instantaneous Phase Detection of Structural Damage*. Springer, Berlin (2005)
51. Marwan, N., Romano, M.C., Thiel, M., Kurths, J.: Recurrence plots for the analysis of complex systems. *Phys. Rep.* **438**(5–6), 237–329 (2007)
52. Bradley, E., Mantilla, R.: Recurrence plots and unstable periodic orbits. *Chaos* **12**(3), 596–600 (2002)
53. Gottwald, A., Melbourne, I.: A new test for chaos in deterministic systems. *Proc. Math. Phys. Eng. Sci.* **460**(2042), 603–611 (2004)
54. Gottwald, G.: On the implementation of the 0–1 test for chaos. **1367**(1), 1–22 (2009). Arxiv preprint [arXiv:0906.1418](https://arxiv.org/abs/0906.1418)
55. Kengne, J.: On the dynamics of Chua’s oscillator with a smooth cubic nonlinearity: occurrence of multiple attractors. *Nonlinear Dyn.* **87**(1), 363–375 (2017)
56. Chen, M., Quan, X., Lin, Y., Bao, B.: Multistability induced by two symmetric stable node-foci in modified canonical Chua’s circuit. *Nonlinear Dyn.* **87**(2), 789–802 (2017)
57. Xiong, L., Yan-Jun, L., Zhang, Y.-F., Zhang, X.-G., Gupta, P.: Design and hardware implementation of a new chaotic secure communication technique. *PLoS ONE* **11**(8), 1–19 (2016)
58. Ruo-Xun, Z., Shi-ping, Y.: Adaptive synchronisation of fractional-order chaotic systems. *Chin. Phys. B* **19**(2), 1–7 (2010)
59. Lao, S., Tam, L., Chen, H., Sheu, L.: Hybrid stability checking method for synchronization of chaotic fractional-order systems. *Abstr. Appl. Anal.* **2014**, 1–11 (2014)
60. Kenfack, G., Tiedeu, A.: Secured transmission of ECG signals: numerical and electronic simulations. *J. Signal Inf. Process.* **04**(02), 158–169 (2013)
61. Chen, D., Liu, C., Cong, W., Liu, Y., Ma, X., You, Y.: A new fractional-order chaotic system and its synchronization with circuit simulation. *Circuits Syst. Signal Process.* **31**(5), 1599–1613 (2012)
62. Chen, D., Cong, W., Iu, H.H.C., Ma, X.: Circuit simulation for synchronization of a fractional-order and integer-order chaotic system. *Nonlinear Dyn.* **73**(3), 1671–1686 (2013)
63. Munoz-Pacheco, J.M., Zambrano-Serrano, E., Felix-Beltran, O., Gomez-Pavon, L.C., Luis-Ramos, A.: Synchronization of PWL function-based 2D and 3D multi-scroll chaotic systems. *Nonlinear Dyn.* **70**(2), 1633–1643 (2012)
64. Lv, M., Wang, C., Ren, G., Ma, J., Song, X.: Model of electrical activity in a neuron under magnetic flow effect. *Nonlinear Dyn.* **85**(3), 1479–1490 (2016)
65. Ma, J., Xinyi, W., Chu, R.: Selection of multi-scroll attractors in Jerk circuits and their verification using Pspice. *Nonlinear Dyn.* **76**, 1951–1962 (2014)